Engineering 6 (2020) 1162–1169

Contents lists available at ScienceDirect

Engineering

journal homepage: www.elsevier.com/locate/eng

Research
Coronavirus Disease 2019—Article

SARS-CoV-2 Entry Factors: *ACE2* and *TMPRSS2* Are Expressed in Peri-Implantation Embryos and the Maternal–Fetal Interface

Wei Chen [a,b,c,d,e,#], Peng Yuan [a,b,c,#], Ming Yang [a,b,c,d,e,#], Zhiqiang Yan [a,b,c,d,e], Siming Kong [a,b,c,d,e], Jie Yan [a,b,c,f,g,h], Xixi Liu [a,c,f], Yidong Chen [a,b,c,d,e], Jie Qiao [a,b,c,d,e,f,g,h,*], Liying Yan [a,b,c,d,f,g,h,*]

[a] *Center for Reproductive Medicine, Department of Obstetrics and Gynecology, Peking University Third Hospital, Beijing 100191, China*
[b] *Key Laboratory of Assisted Reproduction (Peking University), Ministry of Education, Beijing 100191, China*
[c] *Beijing Key Laboratory of Reproductive Endocrinology and Assisted Reproductive Technology, Peking University Third Hospital, Beijing 100191, China*
[d] *Academy for Advanced Interdisciplinary Studies, Peking University, Beijing 100871, China*
[e] *Peking–Tsinghua Center for Life Sciences, Peking University, Beijing 100871, China*
[f] *National Clinical Research Center for Obstetrics and Gynecology, Beijing 100191, China*
[g] *Beijing Advanced Innovation Center for Genomics, Beijing 100871, China*
[h] *Research Units of Comprehensive Diagnosis and Treatment of Oocyte Maturation Arrest, Beijing 100191, China*

ARTICLE INFO

Article history:
Received 30 April 2020
Revised 15 May 2020
Accepted 12 July 2020
Available online 17 August 2020

Keywords:
SARS-CoV-2
ACE2
Vertical transmission
Placenta
Peri-implantation

ABSTRACT

Severe acute respiratory syndrome coronavirus 2 (SARS-CoV-2) has spread throughout the world, leading to large-scale population infection. Angiotensin-converting enzyme 2 (ACE2) is the receptor of both severe acute respiratory syndrome coronavirus (SARS-CoV) and SARS-CoV-2. However, it is still controversial whether vertical transmission exists. In order to investigate the potential risk of SARS-CoV-2 vertical transmission, we explored *ACE2* and *TMPRSS2* (encoding transmembrane protease serine 2) expression patterns in peri-implantation embryos and the maternal–fetal interface using previously published single-cell transcriptome data. The results showed that day 6 (D6) trophectoderm (TE) cells in peri-implantation embryos, as well as syncytiotrophoblast (STB) at 8 weeks of gestation (STB_8W) and extravillous trophoblast (EVT) cells at 24 weeks of gestation (EVT_24W) in the maternal–fetal interface, strongly co-expressed *ACE2* and *TMPRSS2*, indicating a SARS-CoV-2 infection susceptibility. The *ACE2* positive-expressing cells in the three cell types mentioned above were found to share common characteristics, which were involved in autophagy and immune-related processes. *ACE2* showed no gender bias in post-implantation embryos but showed a significant gender difference in D6_TE, D6 primitive endoderm (PE) cells, and *ACE2* positive-expressing STBs. These findings suggest that there may be different SARS-CoV-2 infection susceptibilities of D6 embryos of different genders and during the gestation of different genders. Our results reveal potential SARS-CoV-2 infection risks during embryo transfer, peri-implantation embryo development, and gestation.

1. Introduction

Severe acute respiratory syndrome coronavirus 2 (SARS-CoV-2) has spread throughout the world, with over 10 000 000 confirmed cases and almost 500 000 deaths worldwide according to the WHO report as of June 29, 2020. The zinc metallopeptidase angiotensin-converting enzyme 2 (ACE2) was first discovered in 2000. The expression level of *ACE2* correlates with heart function, hypertension, and diabetes [1,2]. ACE2 is thought to serve as the receptor for both severe acute respiratory syndrome coronavirus (SARS-CoV) and SARS-CoV-2 [3,4], and transmembrane protease serine 2 (TMPRSS2) is a serine protease to prime the SARS-CoV-2 spike (S) protein [5]. Thus, *ACE2* positive-expressing organs are believed to have a high risk of infection [6]. *ACE2* is expressed in lung alveolar epithelial cells, enterocytes of the small intestine [7], a small population of type II alveolar (AT2) cells [8], and respiratory epithelial cells [6]. Furthermore, *ACE2* has been reported to highly express in myocardial cells, epithelial cells of the ileum and

* Corresponding authors.
E-mail addresses: jie.qiao@263.net (J. Qiao), yanliyingkind@aliyun.com (L. Yan).
# These authors contributed equally to this work.

http://dx.doi.org/10.1016/j.eng.2020.07.013

esophagus, proximal tubule cells of the kidney, and bladder urothelial cells [6].

During gestation, the maternal immune system changes to a general state of immunosuppression to prevent repulsion of the fetal allograft [9], which carries an increasing risk of various virus infections [10]. The placenta serves as the foremost barrier against the maternal–fetal transmission of viruses [11]. However, *ACE2* positive-expressing cells have been reported to distribute in syncytiotrophoblasts (STBs), cytotrophoblasts (CTBs) in villi, decidual perivascular cells (dP), decidual stromal cells (dS), and endothelium and vascular smooth muscle cells in the decidua [12,13]. *ACE2* regulates angiotensin (Ang) 1–7 to release into the maternal circulation in STBs, leading to maternal vasculature vasodilation [12]. Meanwhile, previous studies have reported that SARS-CoV and SARS-CoV-2 were not detected in newborn babies delivered from SARS-CoV- and SARS-CoV-2-infected pregnant women [14–16], or in the uteruses of SARS-CoV- and SARS-CoV-2-infected patients [14,17]. Two recent studies claimed that SARS-CoV-2-specific immunoglobulin M (IgM) antibodies were detected in three cases of newborn blood samples [18,19]. Since IgM antibodies cannot generally be transmitted through the placenta to the fetus, and since the production of IgM usually takes 3–7 days after infection, these findings implied that there might be an intrauterine infection, although virus detection of the fetus was negative. Pre-/post-implantation embryos undergo dramatic changes in morphologic and molecular profile [20–22], and embryos are directly exposed to the endometrial cavity in the uterus after zona hatching, which occurs around day 6 (D6) after fertilization [23]. The potential risks for SARS-CoV-2 infection for pre-/post-implantation embryos remains to be elucidated.

To better understand the potential risk of SARS-CoV-2 vertical transmission, we analyzed *ACE2* and *TMPRSS2* expression patterns in pre-implantation embryos, peri-implantation embryos, and the maternal–fetal interface at the single-cell transcriptome level, with the aim of expounding and providing theoretical bases for the possibility of SARS-CoV-2 vertical transmission.

2. Materials and methods

2.1. Data downloading and processing

The pre-implantation embryo data was downloaded from a previously published dataset [24], and the peri-implantation embryo expression data was downloaded from another previously published dataset [22]. The raw data on the pre-implantation embryos was trimmed and mapped to the *Homo sapiens* genome assembly the Genome Reference Consortium Human Genome Build 37 (GRCh37) reference sequence (RefSeq) with STAR [25]. The fragments per kilobase million (FPKM) was calculated to estimate the expression. The peri-implantation embryo data was handled as described in Ref. [22]. The gene expression matrix and related cell-type annotation file of Smart-seq2 (Smart: switching mechanism at 5′ end of the RNA transcript sequencing) single-cell RNA sequencing (scRNA-seq) data of decidual cells and villous cells were respectively downloaded from two previously published datasets [26,27]. The raw count matrix and cell-type annotation file of the droplet scRNA-seq of the human maternal–fetal interface were downloaded from a previously published dataset [27].

2.2. Definition of ACE2 and TMPRSS2 gene positive expression

Cells with gene expression (transcripts per kilobase million, TPM) greater than or equal to 1 are defined as "positive expressing cells" in the Smart-seq2 dataset. For droplet scRNA-seq data, cells with a count greater than 0 are defined as "positive expressing cells."

2.3. Different expression genes and gene ontology analysis

Differentially expressed genes (DEGs) between cells with different expression levels of *ACE2* were identified using the "FindMarkers" function in the "Seurat v3.0" package [28], with the following parameters: "logfc. threshold = log(2), min. pct = 0.4, test.use = 'roc', only.pos = F". Gene ontology (GO) analysis was performed using the "enrichGO" function in "clusterProfiler (3.8.1)" packages [29], with the following parameters: "ont = 'BP', pvalueCutoff = 0.05, pAdjustMethod = 'BH', qvalueCutoff = 0.1, readable = T". We used the R packages "VennDiagram (1.6.20)" and "UpSetR (1.3.3)" to show the relationship among different groups of DEGs, Kyoto Encyclopedia of Genes and Genomes (KEGG) pathways, or GO term lists [30,31]. R (version 3.5.2) was used to carry out all those analyses.

2.4. Embryo and villous sex determination

The sex of each embryo and villous sample was determined by the expression of 15 Y chromosome-specific expressed genes, including: *RBMY2FP*, *RBMY1B*, *TTTY15*, *KDM5D*, *RBMY1J*, *RBMY1F*, *RBMY1D*, *RBMY1E*, *TSPY4*, *TSPY2*, *TSPY8*, *TSPY1*, *RPS4Y1*, *EIF1AY*, and *DDX3Y*. The sex was determined at a whole sample level, so we first calculated the sum expression level of Y chromosome-specific expressed genes at the single-cell level. Embryos with more than 85% cells reached the threshold were defined as male (sum Y chromosome (chrY) gene greater than or equal to 100). Villous sample with more than 65% cells reaching the threshold were defined as male (sum chrY gene greater than or equal to 5 (TPM) in Smart-seq2 cases and sum chrY gene greater than or equal to 1 (scaled count) in droplet cases).

2.5. Statistical analyses

For box-dot plots, the Wilcoxon rank-sum test was performed to determine the significance of differences between two groups. Spearman's correlation coefficient was used to measure the correlation between the expression of *ACE2* and *TMPRSS2* in D6 peri-implantation embryos.

3. Results

3.1. Potential risk of SARS-CoV-2 infection in peri-implantation embryos

Our previous studies have profiled the global transcriptional dynamics of human pre-implantation and peri-implantation embryo cells at multiple consecutive stages [22,24]. *ACE2* is the cell receptor of SARS-CoV-2. In order to investigate the potential infection risk of pre-/peri-implantation embryos, we further analyzed the *ACE2* expression patterns in oocytes and embryos based on our previous studies [22,24]. *ACE2* was found to be expressed through the different stages of pre-implantation embryo development. The expression level of *ACE2* was highest in zygotes; it then decreased sharply from the 4-cell stage and was exhausted at the morula stage. Next, *ACE2* expression was elevated in the blastocyst (Bst) stage (Fig. 1(a)). In peri-implantation embryos, *ACE2* was mainly expressed in day 6 trophectoderm (TE) (D6_TE), day 10 primitive endoderm (PE) (D10_PE), and day 12 PE (D12_PE) (Fig. 1(b)). Since the entry of SARS-CoV-2 into cells depends on the expression of *ACE2* and *TMPRSS2* [5], we also explored *TMPRSS2* expression in peri-implantation embryos. *TMPRSS2* was highly expressed in the TE lineage and the expression

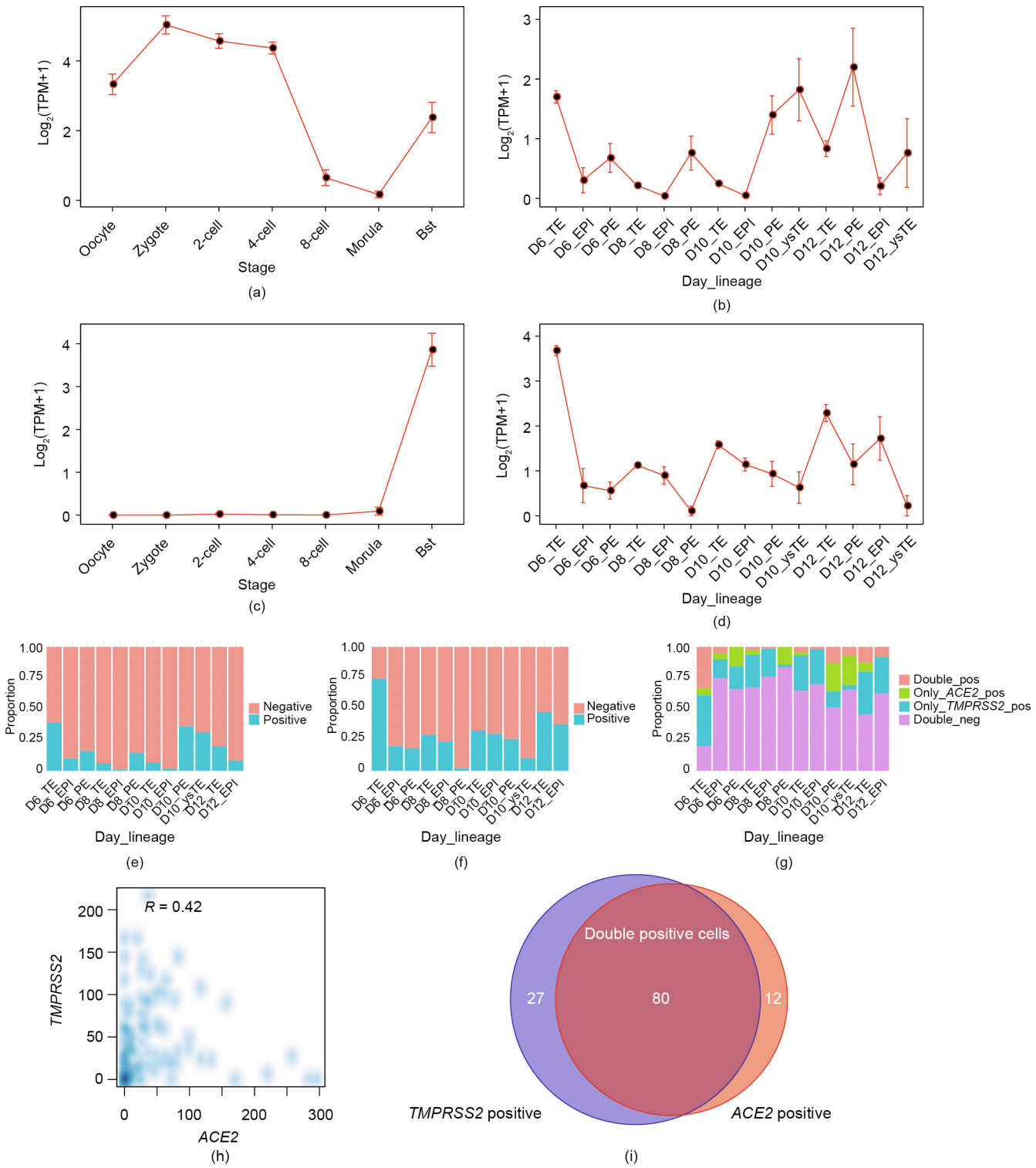

Fig. 1. *ACE2* and *TMPRSS2* expression pattern in pre-implantation and peri-implantation embryos. (a) *ACE2* expression level in different stages of pre-implantation embryos; (b) *ACE2* expression level in different stages of peri-implantation embryos; (c) *TMPRSS2* expression level in different stages of pre-implantation embryos; (d) *TMPRSS2* expression level in different stages of peri-implantation embryos; (e) proportion of *ACE2* positive-and negative-expressing cells in different stages of peri-implantation embryos; (f) proportion of *TMPRSS2* positive- and negative-expressing cells in different stages of peri-implantation embryos; (g) proportion of cells with different expression patterns of *ACE2* and *TMPRSS2* in different stages of peri-implantation embryos (double_pos: cell with both *ACE2* and *TMPRSS2* positive expression; only_*ACE2*_pos: cell with *ACE2* positive expression but not expressing *TMPRSS2*; only_*TMPRSS2*_pos: cell with *TMPRSS2* positive expression but not expressing *ACE2*; double_neg: cell with neither *TMPRSS2* expression nor *ACE2* expression); (h) correlation between the expression of *ACE2* and *TMPRSS2* in D6 peri-implantation embryos (*R* value is the Spearman correlation coefficient); (i) number of cells with both *ACE2* and *TMPRSS2* positive expression in D6 peri-implantation embryos. Bst: blastocyst; EPI: epiblast; ysTE: yolk sac trophectoderm. Error bars represent means ± standard errors.

level of *TMPRSS2* was highest in D6_TE cells (Figs. 1(c) and (d)). Single-cell sequencing enabled us to determine the cell heterogeneity among different developmental stages. We summarized the positive-expressing (TPM ≥ 1) proportion of *ACE2* and *TMPRSS2* at each stage. The proportion of *ACE2* positive-expressing cells was highest in D6_TE cells (38.9%) and the epiblast lineage retained a

low proportion of *ACE2* positive-expressing cells. In accordance with *ACE2* expression levels, the proportion of *ACE2* positive-expressing cells was relatively high in D10_PE cells (Fig. 1(e)). Intriguingly, the proportion of *TMPRSS2* positive-expressing cells was also highest in D6_TE cells (74.1%), while the epiblast (EPI) and PE lineages had relatively low proportion of *TMPRSS2* positive-expressing cells (Fig. 1(f)). Furthermore, we found that the co-expression of *ACE2* and *TMPRSS2* was highest (33.3%) in D6_TE (Fig. 1(g)). Of 194 *ACE2* positive-expressing TE cells, 166 were simultaneously expressing *TMPRSS2*. The correlation between *ACE2* and *TMPRSS2* expression was highest in female D6_TE during peri-implantation embryo development (Fig. 1(h)). Of 92 *ACE2* positive-expressing female TE cells, 80 were simultaneously *TMPRSS2* positive-expressing in female D6_TE (Fig. 1(i)). Taken together, these results indicate that D6 blastocysts are relatively vulnerable to SARS-CoV-2 infection, and a potential risk exists for SARS-CoV-2 infection during peri-implantation embryo development.

3.2. Potential risk of SARS-COV-2 infection in the maternal–fetal interface

To evaluate the potential risk of SARS-CoV-2 vertical transmission in post-implantation development, we then examined the *ACE2* expression level in the maternal–fetal interface based on scRNA-seq data published previously [26,27]. The researchers had profiled the transcriptional characters of various cell types in the maternal–fetal interface, and we adopted the original definition for each cell type. The expression levels of *ACE2* and *TMPRSS2* were highly heterogeneous among the different cell types in the maternal–fetal interface (Figs. S1 and S2 in Appendix A). The results from droplet scRNA-seq data revealed that there was no *ACE2* positive-expressing cell type in maternal peripheral blood. The top four subgroups with the highest proportion of *ACE2* positive-expressing cells were decidual perivascular cells (dP1 and dP2; 1 and 2 mean different cell subtypes), STB and CTB (10%, 5%, 9%, and 5%, respectively; Fig. S3(a) and Table S1). The highest proportions of *ACE2* positive-expressing decidual cell types were in Endo (L) (20% of all five cells) and dP (13% of 84 cells), based on Smart-seq2 data (Fig. 2(a) and Table S2). Despite the lower positive-expressing proportion, *ACE2* was also expressed in decidual natural killer cells (dNK: 1%) and decidual macrophages (dM: 1%) (Table S2). In villi, STB and CTB had the highest *ACE2* positive-expressing cell proportions among all six major types of villous cells in the 8-week group (STB_8W: 41%; CTB_8W: 20%), with an overall positive-expressing proportion of 8.5% (Fig. 2(b) and Table S3). The remarkably increased *ACE2* positive-expressing proportion in STB and CTB might be caused by the detection of low *ACE2* expression level in the cells, which was obtained due to the higher sequencing depth. It is worth noting that the positive-expressing cell proportion in extravillous trophoblasts (EVTs) enriched from the maternal surface of a 24-week placenta (EVT_24W) was 63%, which was much higher than that of EVTs from villous samples at 8 weeks (EVT_8W), at 3% (Fig. 2(b) and Table S3). Similar to *ACE2*, the expression of *TMPRSS2* was detected in the villous and decidual cell types mentioned above, and the highest *TMPRSS2* positive-expressing proportions were in STB_8W, EVT_24W, and epithelial glandular cells (Epi) (26%, 19%, and 19%, respectively; see Figs. S3(b)–(d) and Tables S1–S3). The co-expression of *ACE2* and *TMPRSS2* occurred mainly in STB_8W and EVT_24W (13% and 14%, respectively; see Fig. 2(c) and Table S3), while there was no observation of co-expression in any decidual cells (Fig. 2(d) and Table S2), suggesting that both the STB in villi and the EVT in the decidua are susceptible to SARS-CoV-2. Taken together, these results imply that there is a potential risk of SARS-CoV-2 vertical transmission in pregnancy, due to the existence of *ACE2* and *TMPRSS2* double positive-expressing cells in the maternal–fetal interface.

3.3. Common profile of ACE2 positive-expressing cells among different cell types

As previously mentioned, D6 female TE cells, EVT_24W cells, and STB_8W cells were the top three cell types with the highest risk of SARS-CoV-2 infection. To obtain further understanding of those cells, GO and KEGG pathway enrichment analyses were performed on DEGs between *ACE2* positive-expressing and negative-expressing subtypes in each of these three cell groups (for details, see Tables S4 and S5). Common DEGs, GO terms, and KEGG pathways were found among different lists in the subsequent integration analysis (Figs. 3(a), S4(a), and S4(b)). The processes of the "viral life cycle," "process utilizing autophagic mechanism," and "membrane fusion" were enriched in all three up-regulated DEG groups; the former two were even enriched in all five analyzed groups (Figs. 3(b), S4(c), and S5). Meanwhile, "sphingolipid metabolism" was the common KEGG pathway in three up-regulated groups and "lysosome" was enriched in all five analyzed groups (Figs. 3(c) and S6). Many studies have also reported that the mechanisms involved in the sphingolipid metabolism and lysosomal degradation pathway took part in the processes of virus infections and related cell response [32–35]. These findings suggest that the *ACE2* positive-expressing and *ACE2* negative-expressing cells are probably in a different state when responding to viral infection, aside from having a different sensitivity to SARS-CoV-2. This hypothesis was further supported by our observations of immune and virus-related processes in GO enrichment in all three cell groups (Fig. S7(a)). The DEGs in these terms contained many interferon-stimulated genes (ISGs), which have already been reported, and genes that are involved in inflammation and defense against viral infection (Figs. S7(b)–(g)). Furthermore, *ACE2* positive-expressing and *ACE2* negative-expressing EVT_24W or STB_8W cells might have different metabolisms, as revealed by the metabolic processes/pathways, "regulation of cholesterol metabolic process" in GO and "steroid biosynthesis" in KEGG, for example (Figs. S4(c) and S6(a)). There were 12 common up-regulated expression DEGs in all three *ACE2* positive subtypes (Fig. 3(d)), such as *MDK*, *UGCG*, and *RAB25*, which are implicated in the processes of inflammatory response, cell proliferation, cell growth, and cell migration. Overall, these results indicate that the *ACE2* positive-expressing cells in D6 female TE cells and the EVT_24W and STB_8W cell groups show certain common characteristics in comparison with the *ACE2* negative-expressing cells, which suggest a general profile of sensitivity to SARS-CoV-2 in early and later TE lineage cells.

3.4. Gender bias in ACE2 expression of peri-implantation embryos and villi

As the *ACE2* gene is located in the X chromosome and escapes from chromosome inactivation [36], we speculated that different expression levels of *ACE2* might exist, as the X chromosome copy number differs in male and female embryos. After comparing embryos of the different genders, we found that the *ACE2* expression level was high in D6 female TE and PE cells, but not in the latter development stages of post-implantation (Fig. 4(a)). The *TMPRSS2* expression showed no significant difference between male and female embryos, except for D12_TE cells during peri-implantation development (Fig. 4(b)). We further analyzed the *ACE2* and *TMPRSS2* expression levels in subsequent villous cells of different genders. Three male villous samples were identified in droplet data. The *ACE2* expression level showed a significant gender difference in *ACE2* positive-expressing STB and CTB, while

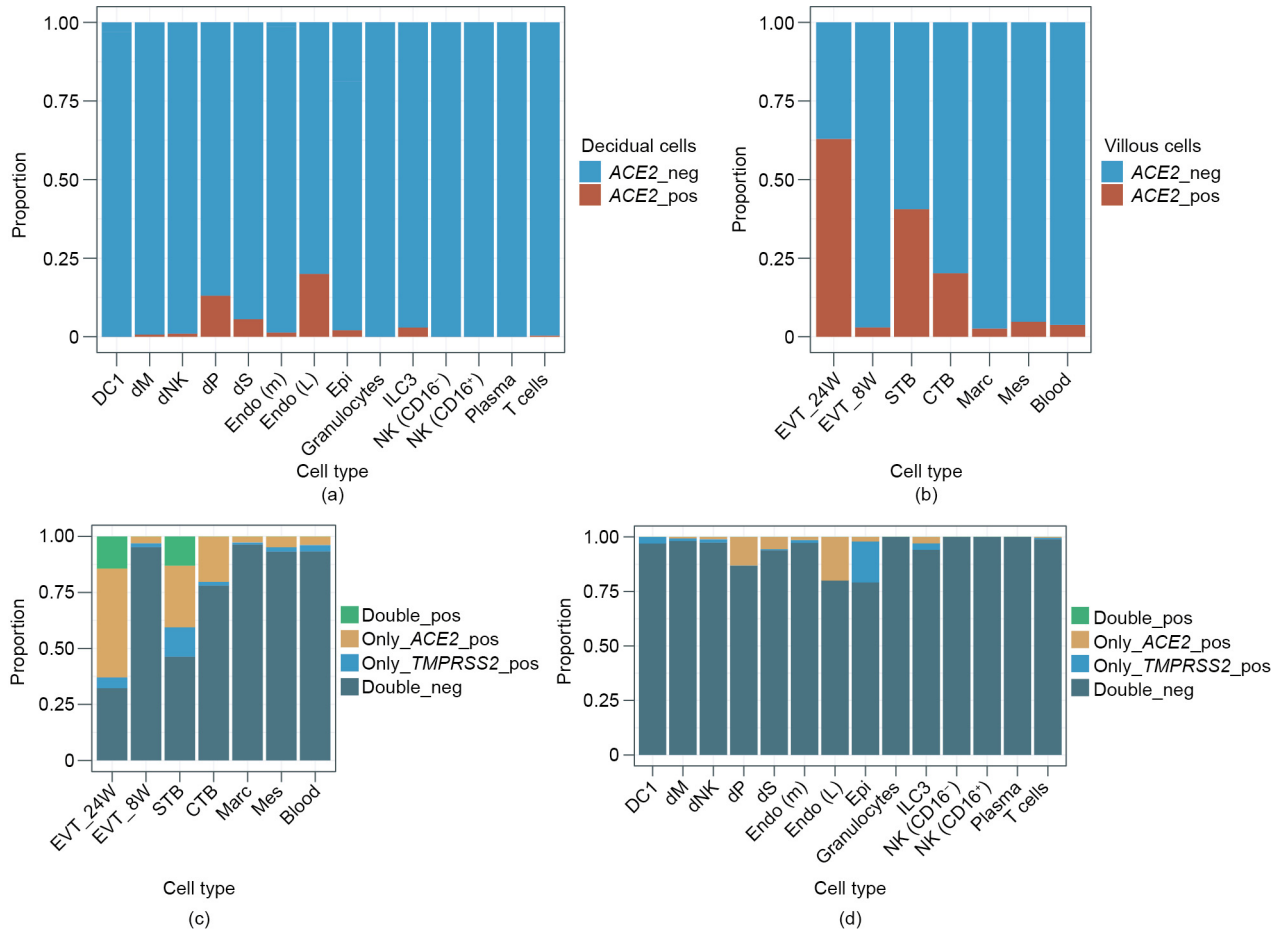

Fig. 2. *ACE2* and *TMPRSS2* expression pattern in the maternal–fetal interface. (a) Proportion of *ACE2* positive- and negative-expressing cells in different cell types in decidual cells; (b) proportion of *ACE2* positive- and negative-expressing cells in different cell types in villous cells; (c) proportion of cells with different expression patterns of *ACE2* and *TMPRSS2* in villous cells; (d) proportion of cells with different expression patterns of *ACE2* and *TMPRSS2* in decidual cells. DC: dendritic cells; dM: decidual macrophages; dNK: decidual natural killer (NK) cells; dP: decidual perivascular cells; dS: decidual stromal cells; Endo: endothelial cells; Epi: epithelial glandular cells; ILC: innate lymphocyte cell; STB: syncytiotrophoblast; CTB: villous cytotrophoblast; EVT: extravillous trophoblast; Marc: fetal macrophages (also called Hofbauer cells); Mes: mesenchymal stromal cells; L: lymphatic; m: maternal; p: proliferative; CD16 is also known as FcγRIII, belonging to the immunoglobulin superfamily (IgSF), and $CD16^{+/-}$ means CD16 positive- or negative-expressing cells in immunofluorescence staining in flow cytometry; T cell: thymus-dependent lymphocyte.

the *TMPRSS2* expression level showed no gender bias in *TMPRSS2* positive-expressing cells (Figs. 4(c), 4(d), and S8(a)). Only one male villous sample was identified in Smart-seq2 data, and there was no significant gender bias in both STB_8W and EVT_8W, in accordance with the post-implantation TE cells (Figs. S8(b)–(d)). In conclusion, *ACE2* showed no global gender bias in post-implantation embryos, but was highly expressed in D6 female TE and PE cells, along with a gender difference in *ACE2* positive-expressing STB and CTB. These findings indicate that there may be different SARS-CoV-2 infection susceptibilities in D6 embryos of different genders, as well as during gestation.

4. Discussion

The COVID-19 pandemic has posed huge challenges to global public health. Pregnant patients are subject to special attention due to concerns about compounding pregnancy complications and potential negative influences on fetal development *in utero*. Whether SARS-CoV-2 can infect the embryo or placenta and disturb the establishment or maintenance of pregnancy, and the possible existence of vertical transmission, are hot topics. In this study, we comprehensively investigated the single-cell transcriptome data of pre-/post-implantation embryos at consecutive stages and the maternal–fetal interface to clarify the expression profiles of *ACE2* and *TMPRSS2*, as well as other molecular signatures involved in SARS-CoV-2 infection. We found that *ACE2* and *TMPRSS2* were strongly co-expressed in D6_TE, STB_8W in villi, and EVT_24W cells in the decidua. Common DEGs, GO terms, and KEGG pathways were observed among the top three cell types with the highest potential risk of SARS-CoV-2 infection, which indicated that *ACE2* positive-expressing cells shared conserved changes involved in the autophagy-lysosome system, and immune and virus-related processes when compared with *ACE2* negative-expressing cells. Furthermore, we revealed that *ACE2* was highly expressed in D6 female TE and PE cells, along with a significant gender difference in *ACE2* positive-expressing STB. Collectively, this research presents an *ACE2* expression landscape in peri-implantation embryos and the maternal–fetal interface for the first time at the single-cell transcriptome level, and suggests a potential risk of SARS-CoV-2 vertical transmission during the peri-implantation period and pregnancy.

ACE2 was found to be expressed in peri-implantation embryos. The *ACE2* positive-expressing cell proportion was highest in the D6_TE cells of peri-implantation embryos, although other lineages showed low expression. This was consistent with the *TMPRSS2* positive-expressing cell proportion and the co-positive-expressing cell proportion in D6_TE cells, indicating a relatively

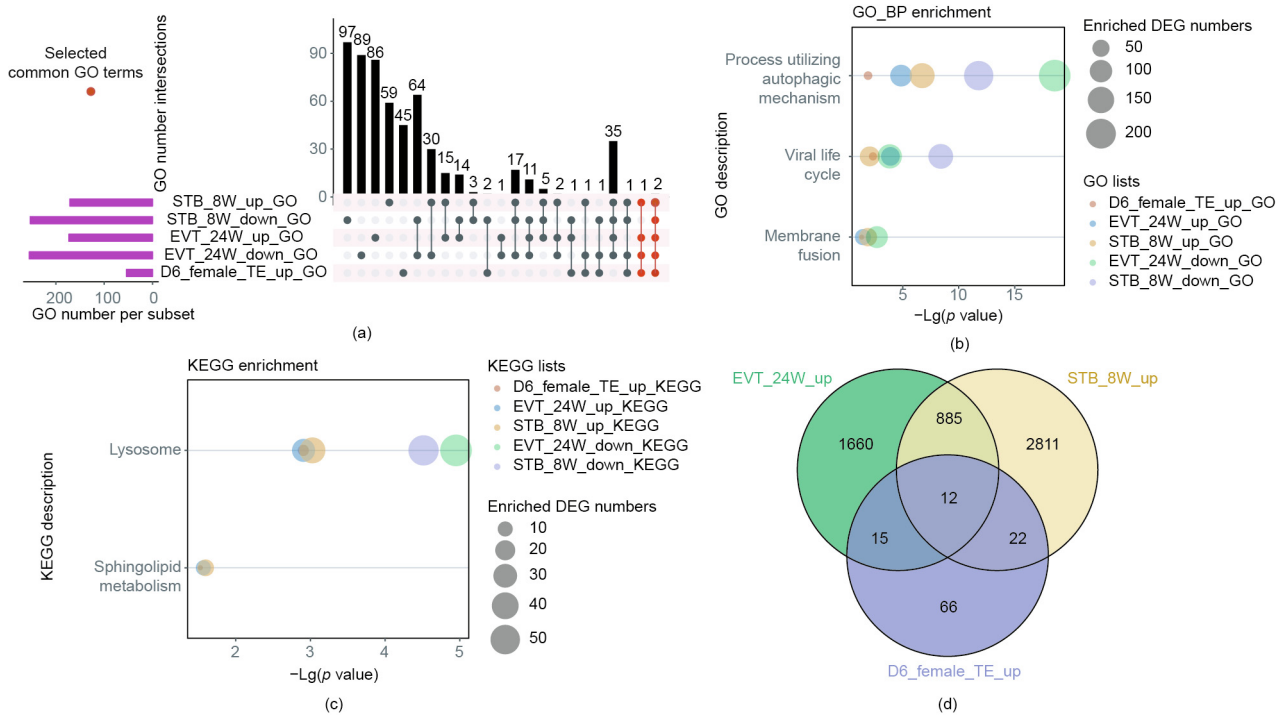

Fig. 3. Differentially expressed genes and enriched biological processes/pathways between *ACE2* positive-expressing and *ACE2* negative-expressing expression cells in D6 female TE and in EVT_24W and STB_8W cell groups. (a) Number of cell-type specific or inter-cell-type common biological processes in GO enrichment among D6 female TE, and EVT_24W and STB_8W cell groups; (b) common enriched GO terms of all three up-regulated DEGs among D6 female TE, and EVT_24W and STB_8W cell groups; (c) common enriched KEGG pathway of all three up-regulated DEGs among D6 female TE, and EVT_24W and STB_8W cell groups; (d) number of common DEGs in all three up-regulated DEGs among D6 female TE, and EVT_24W and STB_8W cell groups.

high susceptibility to SARS-CoV-2 infection in D6 embryos. Nevertheless, since *ACE2* displayed a relatively low expression level, the possibility of infection may still exist at other developmental stages. These findings also suggest a potential infection risk during embryo transplantation in clinic *in vitro* fertilization (IVF).

In the maternal–fetal interface, the data showed that CTB, STB, EVT, and dP cells had a high *ACE2* positive-expressing proportion; the highest co-positive-expressing proportion of *ACE2* and *TMPRSS2* occurred in STB_8W and EVT_24W. It is known that CTB derives from TE and then differentiates into STB and EVT, with the former being infiltrated by maternal blood and the latter invading uterine spiral arteries [23,37]. In a previously published study, SARS-CoV-2 was detected in three of 307 blood samples collected from 205 patients [38], although the detection proportion was low. STB were directly exposed to the mother's blood, so the virus in the blood would mainly infect STB. EVT also showed a high infection possibility *in utero* for part of EVT serving as a kind of blood vessel wall cell and located in the decidua. Although the *ACE2* positive-expressing cell proportion was much higher in EVT_24W than in EVT_8W, the various risks of vertical transmission at the different stages of pregnancy have yet to be assessed. Taken together, these results indicate a potential risk of SARS-CoV-2 vertical transmission during gestation.

Although there is no direct evidence for SARS-CoV-2 vertical transmission, two studies published in *The Journal of the American Medical Association* (*JAMA*) reported three cases of newborn babies with positive SARS-CoV-2 IgM antibodies, suggesting that vertical transmission may exist. Moreover, our study found that *ACE2* and *TMPRSS2* co-positive-expressing cells were present in the maternal–fetal interface, providing a theoretical possibility of SARS-CoV-2 vertical transmission during gestation. If pregnant women are infected with SARS-CoV-2 in the first trimester, the health monitoring of the mother and baby should be strengthened. Intrauterine SARS-CoV-2 transmission might directly affect the clinical therapeutic schedules for infected pregnant women. With this research, we hope to provide theoretical bases for the clinical diagnosis and treatment of pregnant women. As for the existence of vertical transmission, further accumulation of clinical cases and more confirmation from basic research are necessary.

We also analyzed the differentially expressed genes between *ACE2* positive- and negative-expressing cells in three cell groups with a high risk of SARS-CoV-2: D6 female TE, EVT_24W, and STB_8W cell groups. We found that some common virus-related and cell response processes and pathways were enriched in these three cell types. The GO term "process utilizing an autophagic mechanism" and the KEGG pathway "lysosome" were enriched in all five analyzed groups. As a lysosome-dependent process, autophagy has been thought to play an important role in maintaining cellular homeostasis and defending against viral infection [39,40]. Many studies suggest that viruses may hijack the conserved autophagic machinery during infection for their advantage [41,42]. Our results revealed that the *ACE2* positive-expressing cells in TE lineage cells at different development stages shared some common changes involved in the autophagy process, when compared with *ACE2* negative-expressing cells. This finding supports the view that it is reasonable to set the autophagy process as a target in therapeutic strategies for SARS-CoV-2 infection [43]. We also revealed that the DEGs in these three cell groups showed enrichment in the biological processes of the immune and defense responses to the virus. Many ISGs were involved in the DEGs in those GO terms. Ziegler et al. [44] indicated that *ACE2* was actually a neglected ISG. It partly interprets the coordinated changes of *ACE2* and ISGs observed in three TE lineage cells.

X chromosome inactivation (XCI) is a crucial epigenetic mechanism to balance X chromosome expression dosage between XY males and XX females. As an escape gene, *ACE2* is reported to show

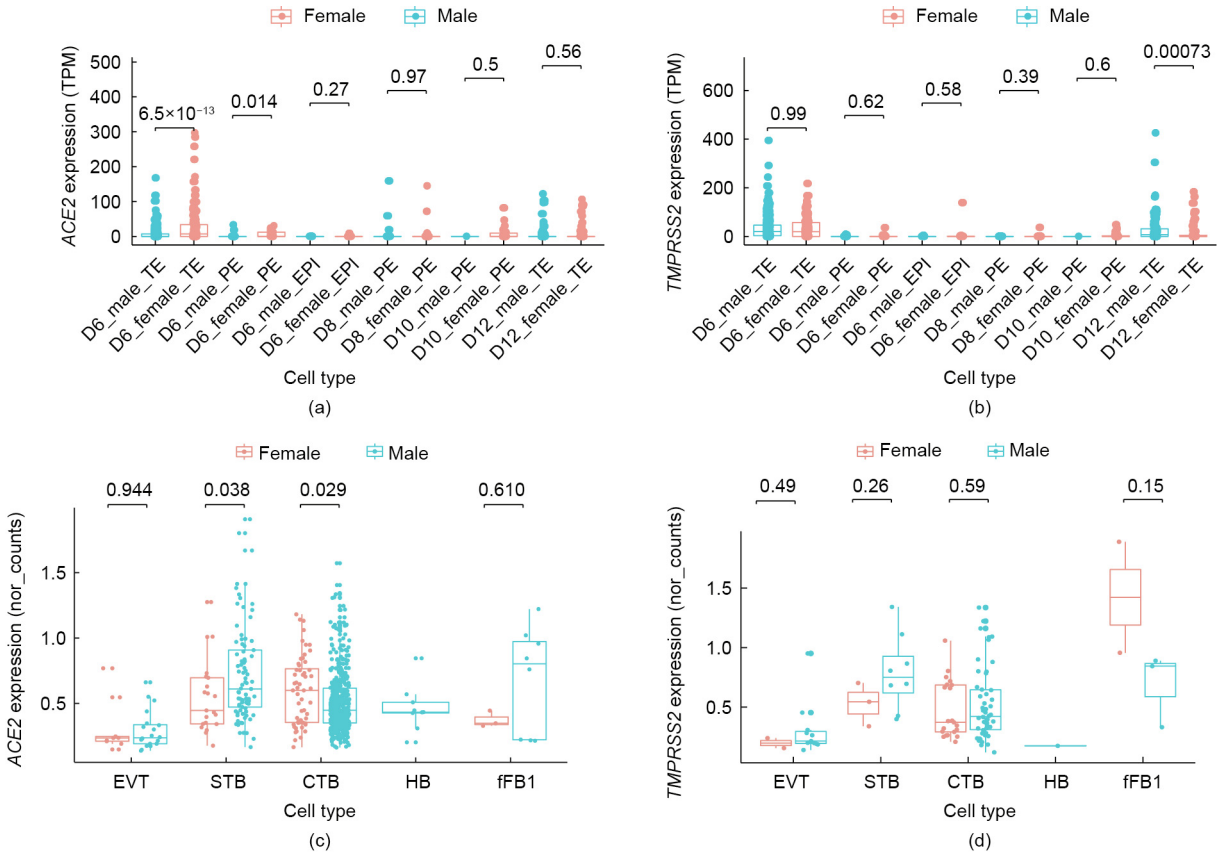

Fig. 4. *ACE2* expression level in peri-implantation embryos and villous cells with different genders. (a) *ACE2* expression in all cells in different stages of peri-implantation embryos of different genders; (b) *TMPRSS2* expression in all cells in different stages of peri-implantation embryos in different genders; (c) *ACE2* expression in *ACE2* positive-expressing villous cells of different genders in droplet data analysis; (d) *TMPRSS2* expression in *TMPRSS2* positive-expressing villous cells of different genders in droplet data analysis. Nor_count: normalized counts; HB, Hofbauer cells; fFB1, fetal fibroblasts 1. The *p*-value between two gender groups was determined by the Wilcoxon rank-sum test.

a heterogeneous sex bias [36]. In this study, we found that the *ACE2* expression level in D6 female TE cells was significantly higher than in male, albeit not in the later development stages. *ACE2* positive-expressing STB and CTB also showed significant differences between female and male samples. These findings suggest a gender bias in the risk of SARS-CoV-2 vertical transmission during the peri-implantation period and gestation. These results also imply that *ACE2* might not escape X-inactivation in human post-implantation embryos, which enhances our knowledge about XCI during early embryo development.

5. Conclusions

Although IgM antibodies have been detected in blood samples in neonates, it is still controversial whether SARS-CoV-2 can be transmitted *in utero*. More definitive evidence is still urgently needed to validate the vertical transmission of SARS-CoV-2. In this study, we provided theoretical bases for the vertical transmission possibility of SARS-CoV-2 infection during peri-implantation embryo development and gestation, and provided recommendations for SARS-CoV-2-infected women during pregnancy or who are preparing for pregnancy.

Acknowledgements

We show our admiration and gratitude to those people who are fighting on the front line of defense of SARS-CoV-2. This work was supported by the Peking University Health Science Center (BMU2020HKYZX001), the Chinese Academy of Engineering (2020-KYGG-01-06), and the National Key Research and Development Program of China (2018YFC1004000 and 2019YFA0801400).

Authors' contribution

Wei Chen, Peng Yuan, and Ming Yang wrote the manuscript. Wei Chen and Peng Yuan performed bioinformatic analysis. Zhiqiang Yan, Siming Kong, Jie Yan, Xixi Liu, and Yidong Chen were helpful for the discussion of this study. Jie Qiao and Liying Yan developed the study conception and designs. All the authors have read and approved the final manuscript.

Compliance with ethics guidelines

Wei Chen, Peng Yuan, Ming Yang, Zhiqiang Yan, Siming Kong, Jie Yan, Xixi Liu, Yidong Chen, Jie Qiao, and Liying Yan declare that they have no conflict of interest or financial conflicts to disclose.

Appendix A. Supplementary data

Supplementary data to this article can be found online at https://doi.org/10.1016/j.eng.2020.07.013.

References

[1] Zisman LS, Keller RS, Weaver B, Lin Q, Speth R, Bristow MR, et al. Increased angiotensin-(1–7)-forming activity in failing human heart ventricles: evidence for upregulation of the angiotensin-converting enzyme homologue ACE2. Circulation 2003;108(14):1707–12.

[2] Tikellis C, Johnston CI, Forbes JM, Burns WC, Burrell LM, Risvanis J, et al. Characterization of renal angiotensin-converting enzyme 2 in diabetic nephropathy. Hypertension 2003;41(3):392–7.

[3] Turner AJ, Hiscox JA, Hooper NM. ACE2: from vasopeptidase to SARS virus receptor. Trends Pharmacol Sci 2004;25(6):291–4.

[4] Zhou P, Yang XL, Wang XG, Hu B, Zhang L, Zhang W, et al. A pneumonia outbreak associated with a new coronavirus of probable bat origin. Nature 2020;579(7798):270–3.

[5] Hoffmann M, Kleine-Weber H, Schroeder S, Krüger N, Herrler T, Erichsen S, et al. SARS-CoV-2 cell entry depends on ACE2 and TMPRSS2 and is blocked by a clinically proven protease inhibitor. Cell 2020;181(2). 271–80.e8.

[6] Zou X, Chen K, Zou J, Han P, Hao J, Han Z. Single-cell RNA-seq data analysis on the receptor ACE2 expression reveals the potential risk of different human organs vulnerable to 2019-nCoV infection. Front Med 2020;14(2):1–8.

[7] Hamming I, Timens W, Bulthuis MLC, Lely AT, Navis GJ, van Goor H. Tissue distribution of ACE2 protein, the functional receptor for SARS coronavirus. A first step in understanding SARS pathogenesis. J Pathol 2004;203(2):631–7.

[8] Qi F, Qian S, Zhang S, Zhang Z. Single cell RNA sequencing of 13 human tissues identify cell types and receptors of human coronaviruses. Biochem Bioph Res Co 2020;526(1):135–40.

[9] Aghaeepour N, Ganio EA, Mcilwain D, Tsai AS, Tingle M, Van Gassen S, et al. An immune clock of human pregnancy. Sci Immunol 2017;2(15):eaan2946.

[10] Kourtis AP, Read JS, Jamieson DJ. Pregnancy and infection. N Engl J Med 2014;370(23):2211–8.

[11] Delorme-Axford E, Sadovsky Y, Coyne CB. The placenta as a barrier to viral infections. Annu Rev Virol 2014;1(1):133–46.

[12] Pringle KG, Tadros MA, Callister RJ, Lumbers ER. The expression and localization of the human placental prorenin/renin-angiotensin system throughout pregnancy: roles in trophoblast invasion and angiogenesis? Placenta 2011;32(12):956–62.

[13] Li M, Chen L, Zhang J, Xiong C, Li X. The SARS-CoV-2 receptor ACE2 expression of maternal–fetal interface and fetal organs by single-cell transcriptome study. PLoS ONE 2020;15(4):e0230295.

[14] Ng PC, Leung CW, Chiu WK, Wong SF, Hon EK. SARS in newborns and children. Biol Neonate 2004;85(4):293–8.

[15] Jeong SY, Sung SI, Sung JH, Ahn SY, Kang ES, Chang YS, et al. MERS-CoV infection in a pregnant woman in Korea. J Korean Med Sci 2017;32(10):1717–20.

[16] Zhang Q, Ding Y, Hou J, He L, Huang Z, Wang H, et al. Detection of severe acute respiratory syndrome (SARS)-associated coronavirus RNA in autopsy tissues with in situ hybridization. J First Mil Med Univ 2003;23(11):1125–7. Chinese.

[17] Ding Y, He L, Zhang Q, Huang Z, Che X, Hou J, et al. Organ distribution of severe acute respiratory syndrome (SARS) associated coronavirus (SARS-CoV) in SARS patients: implications for pathogenesis and virus transmission pathways. J Pathol 2004;203(2):622–30.

[18] Zeng H, Xu C, Fan J, Tang Y, Deng Q, Zhang W, et al. Antibodies in infants born to mothers with COVID-19 pneumonia. JAMA 2020;323(18):1848–9.

[19] Dong L, Tian J, He S, Zhu C, Wang J, Liu C, et al. Possible vertical transmission of SARS-CoV-2 from an infected mother to her newborn. JAMA 2020;323(18):1846–8.

[20] Zhu P, Guo H, Ren Y, Hou Y, Dong J, Li R, et al. Single-cell DNA methylome sequencing of human preimplantation embryos. Nat Genet 2018;50(1):12–9.

[21] Xu Q, Xie W. Epigenome in early mammalian development: inheritance, reprogramming and establishment. Trends Cell Biol 2018;28(3):237–53.

[22] Zhou F, Wang R, Yuan P, Ren Y, Mao Y, Li R, et al. Reconstituting the transcriptome and DNA methylome landscapes of human implantation. Nature 2019;572(7771):660–4.

[23] Hui P. Developmental biology of the placenta. In: Hui P, editor. Gestational trophoblastic disease: diagnostic and molecular genetic pathology. New York: Springer New York; 2012. p. 15–39.

[24] Yan L, Yang M, Guo H, Yang L, Wu J, Li R, et al. Single-cell RNA-Seq profiling of human preimplantation embryos and embryonic stem cells. Nat Struct Mol Biol 2013;20(9):1131–9.

[25] Dobin A, Davis CA, Schlesinger F, Drenkow J, Zaleski C, Jha S, et al. STAR: ultrafast universal RNA-seq aligner. Bioinformatics 2013;29(1):15–21.

[26] Liu Y, Fan X, Wang R, Lu X, Dang Y-L, Wang H, et al. Single-cell RNA-seq reveals the diversity of trophoblast subtypes and patterns of differentiation in the human placenta. Cell Res 2018;28(8):819–32.

[27] Vento-Tormo R, Efremova M, Botting RA, Turco MY, Vento-Tormo M, Meyer KB, et al. Single-cell reconstruction of the early maternal–fetal interface in humans. Nature 2018;563(7731):347–53.

[28] Stuart T, Butler A, Hoffman P, Hafemeister C, Papalexi E, Mauck WM, et al. Comprehensive integration of single-cell data. Cell 2019;177(7):1888–902.e21.

[29] Yu G, Wang LG, Han Y, He QY. clusterProfiler: an R package for comparing biological themes among gene clusters. Omics 2012;16(5):284–7.

[30] Chen H, Boutros PC. VennDiagram: a package for the generation of highly-customizable Venn and Euler diagrams in R. BMC Bioinf 2011;12(1):1–7.

[31] Conway JR, Lex A, Gehlenborg N. UpSetR: an R package for the visualization of intersecting sets and their properties. Bioinformatics 2017;33(18):2938–40.

[32] Li C, Zhu Z, Du X, Cao W, Yang F, Zhang X, et al. Foot-and-mouth disease virus induces lysosomal degradation of host protein kinase PKR by 3C proteinase to facilitate virus replication. Virology 2017;509:222–31.

[33] Spence JS, He R, Hoffmann HH, Das T, Thinon E, Rice CM, et al. IFITM3 directly engages and shuttles incoming virus particles to lysosomes. Nat Chem Biol 2019;15(3):259–68.

[34] Goodwin CM, Xu S, Munger J. Stealing the keys to the kitchen: viral manipulation of the host cell metabolic network. Trends Microbiol 2015;23(12):789–98.

[35] Martín-Acebes MA, Merino-Ramos T, Blázquez AB, Casas J, Escribano-Romero E, Sobrino F, et al. The composition of West Nile virus lipid envelope unveils a role of sphingolipid metabolism in flavivirus biogenesis. J Virol 2014;88(20):12041–54.

[36] Tukiainen T, Villani AC, Yen A, Rivas MA, Marshall JL, Satija R, et al. Landscape of X chromosome inactivation across human tissues. Nature 2017;550(7675):244–8.

[37] Windsperger K, Dekan S, Pils S, Golletz C, Kunihs V, Fiala C, et al. Extravillous trophoblast invasion of venous as well as lymphatic vessels is altered in idiopathic, recurrent, spontaneous abortions. Hum Reprod 2017;32(6):1208–17.

[38] Wang W, Xu Y, Gao R, Lu R, Han K, Wu G, et al. Detection of SARS-CoV-2 in different types of clinical specimens. JAMA 2020;323(18):1843–4.

[39] Choi Y, Bowman JW, Jung JU. Autophagy during viral infection—a double-edged sword. Nat Rev Microbiol 2018;16(6):341–54.

[40] Eskelinen EL, Saftig P. Autophagy: a lysosomal degradation pathway with a central role in health and disease. Biochim Biophys Acta 2009;1793(4):664–73.

[41] Lee YR, Lei HY, Liu MT, Wang JR, Chen SH, Jiang-Shieh YF, et al. Autophagic machinery activated by dengue virus enhances virus replication. Virology 2008;374(2):240–8.

[42] De Haan CA, Reggiori F. Are nidoviruses hijacking the autophagy machinery?. Autophagy 2008;4(3):276–9.

[43] Yang N, Shen HM. Targeting the endocytic pathway and autophagy process as a novel therapeutic strategy in COVID-19. Int J Biol Sci 2020;16(10):1724–31.

[44] Ziegler CGK, Allon SJ, Nyquist SK, Mbano IM, Miao VN, Tzouanas CN, et al. SARS-CoV-2 receptor ACE2 is an interferon-stimulated gene in human airway epithelial cells and is detected in specific cell subsets across tissues. Cell 2020;181(5):1016–35.e19.